

INFLUENCE OF Al ON HIGH TEMPERATURE SULFIDATION OF AN Fe-25Cr ALLOY IN H₂S-H₂ GAS MIXTURES^①

Qi, Huibin Zhu, Rizhang

*Department of Surface Science and Corrosion Engineering,
University of Science and Technology Beijing, Beijing 100083, China*

Wang, Shujuan

Northeastern University, Shenyang 110006, China

ABSTRACT

The effects of 5 wt.-% Al and 10 wt.-% Al on the sulfidation behaviour of the Fe-25Cr alloy in H₂S-H₂ gas mixtures in the temperature range of 700~900 °C has been studied. The sulfidation resistance of Fe-25Cr was improved and the sulfide scale morphologies, composition and structure of Fe-25Cr changed remarkably. The sulfidation kinetics of the alloys with aluminium obeyed basically the parabolic law after an initial period of reaction time. The sulfidation mechanism of the Fe-Cr-Al alloy has been proposed.

Key words: Al Fe-25Cr H₂S-H₂ gas mixtures sulfidation

1 INTRODUCTION

The high temperature sulfidation of metallic materials is an important and common corrosion type in the petrochemistry, the liquefaction and gasification of coal and the power plant. The gas mixture of H₂S-H₂ is a typical environment of sulfidation^[1]. The sulfidation resistance of the iron-base alloys bearing chromium is poor in both the sulfur vapour and the H₂S-H₂ gas mixtures^[2-5]. Whether the aluminium, as a ternary alloying element, can be able to enhance the sulfidation resistance of the iron-base alloys like the case that the aluminium acts in their oxidation or not is an interesting problem^[6-10]. In the present paper, the influences of two aluminium contents on the

sulfidation kinetics of Fe-25Cr in H₂S-H₂ gas mixtures with the sulfur pressures of 10⁻³~1 Pa at 700~900 °C has been studied. The sulfidation mechanism of the Fe-Cr-Al alloy is discussed.

2 EXPERIMENTAL

2.1 Alloys

The nominal composition of experimental materials were Fe-25Cr-5Al, Fe-25Cr-10Al, and Fe-25Cr. Their Cr contents (wt.-%) were 24.43, 24.31, 24.49, Al contents 4.70, 9.60, 0.00 and C contents 0.014, 0.01, 0.018, respectively. The ingots were hot rolled into bars of diameters of about 15 mm. The alloys have been annealed at 750 °C for 1 h. The dimensions of

① Financially supported by the National Natural Science Foundation of China and the Chinese Corrosion Science Laboratory; manuscript received Sept. 23, 1992

specimen was $d 12 \text{ mm} \times 1 \text{ mm}$. In order to suspend the specimen a tiny hole of a diameter of 1.5 mm was drilled near its edge. The specimen surface was abraded to 1000 grit emery paper. Prior to use the specimen was repolished to remove the thin oxide film possibly formed on the surface at room temperature and rinsed in acetone.

2.2 Apparatus

In order to obtain the sulfidation kinetics accurately a quartz spring thermobalance suitable for the experiments with highly corrosive agents similar to that in ref. 10 was used.

2.3 Experimental Process

After the sample was suspended under the spring, the sealed reaction chamber was vacuumed by a rotary pump and filled with H_2 of high purity. This process was repeated several times. Then the chamber was filled with the $\text{H}_2\text{S}-\text{H}_2$ gas mixture of a controlled partial pressure ratio continuously. The total pressure of the gas was $1.013 \times 10^5 \text{ Pa}$. When the furnace reached the reaction temperature, it was lifted up to ensure the specimen located in its center. The elongation of the spring was recorded after 5 min.

The sulfide scales were observed and analysed by a scanning electron microscopy (SEM), energy-dispersive X-ray analysis (EDAX), electron-probe microanalysis (EPMA) and X-ray diffraction (XRD).

3 RESULTS

3.1 Sulfidation Kinetics

Fig. 1 shows the sulfidation kinetics of Fe-25Cr-5Al and Fe-25Cr-10Al at different temperatures and different sulfur pressures. The curves were drawn according to the fol-

lowing parabolic law.

$$\left(\frac{\Delta M}{A}\right)^2 = K_p t + C$$

where K_p is the parabolic constant. The weight-gain unit is $\text{mg} \cdot \text{cm}^{-2}$.

It can be concluded from Fig. 1 that the sulfidation kinetics of the two aluminium bearing alloys followed basically an incubation + parabolic law. When changing the temperature at a constant P_{S_2} , the weight-gain and the sulfidation rate of both alloys increased notably with the increase of temperature. In the other hand, when changing the sulfur pressure at 800 °C, the sulfidation rate of the 10 wt.-% Al alloy increased with the increase of P_{S_2} . So did the 5 wt.-% Al alloy in the initial period of reaction after this period of time the tendency of some curves changed and the weight-gain lost its consistence with P_{S_2} . A turn appeared on the weight-gain v. s. time curve is a characteristic of the sulfidation kinetics for the 5 wt.-% Al alloy, especially at higher temperatures and sulfur pressures, this phenomenon is even more prominent (Fig. 1 (a), (b)).

It can be found from Fig. 1 (c) and 1 (d) by careful observation that the parabolic law of the 10 wt.-% Al alloy after the incubation was not a single one. Two or three different parabolic laws appeared and the parabolic constant increased with time. A similar phenomenon was observed in the sulfidation process for the Fe-25Cr alloy under the same conditions^[3]. In Table 1 the two parabolic constants of the 10 wt.-% Al alloy at 800 °C and different sulfur pressures are listed.

To compare the sulfidation rates of all tested alloys, their second parabolic constants at 700~900 °C and $P_{\text{S}_2} = 10^{-2} \text{ Pa}$ are listed in Table 2.

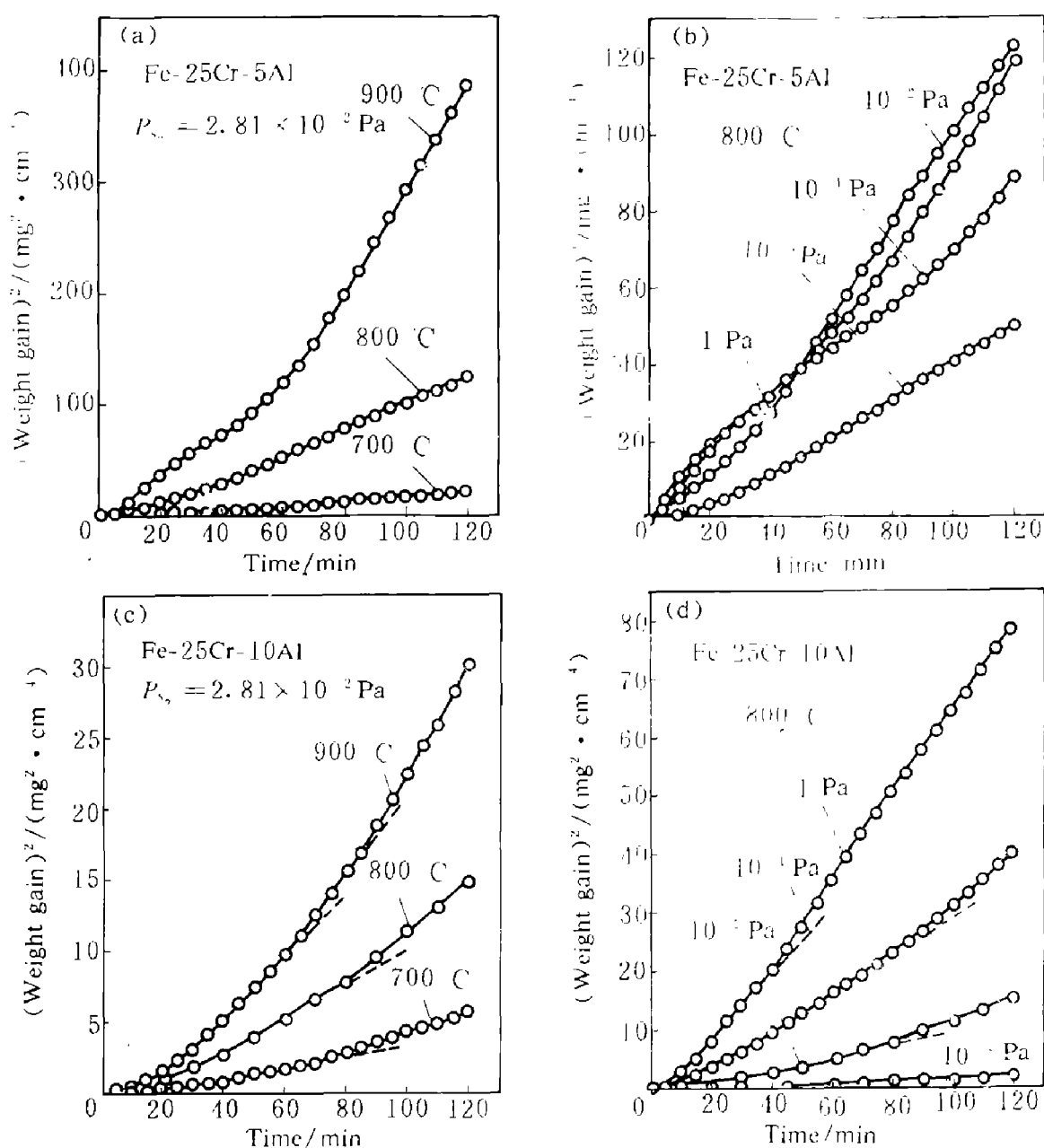


Fig. 1 The sulfidation parabolic curves for Fe-25Cr-5Al and Fe-25Cr-10Al

3.2 Sulfide Morphologies, Structure and Composition

Fig. 2 shows the typical sulfide surface morphologies of Fe-25Cr-5Al and -10Al. Their feature is that the flake sulfide grain grew vertically or by a little angle of inclination from the sample surface. The surface morphologies are dependent on temperature. The higher the temperature, the larger the grain and the more smooth the sulfide sur-

face. It can be found from EDAX that the surface sulfide scale was mainly composed of S, Fe and some Cr and Al. The contents of Cr and Al decreased with increases of the temperature, the sulfur pressure and reaction time, respectively.

XRD result indicated that the sulfide phases of Fe-25Cr-5Al and -10Al could be concluded as follows: Fe_3S_2 , Cr_7S_8 , $\text{Fe-Cr}_7\text{S}_8$ and some trace Al_2S_3 . In every phase there were some other doping elements.

Table 1 Two parabolic constants K_p of Fe-25Cr-10Al at 800 °C and different sulfur pressures

P_{S_2} /Pa	K_p /g ² ·cm ⁻¹ ·s ⁻¹	
	1st parab. const.	2nd parab. const.
2.29×10^{-3}	2.92×10^{-10}	3.55×10^{-10}
2.81×10^{-2}	2.14×10^{-9}	2.98×10^{-9}
2.29×10^{-1}	5.73×10^{-9}	7.35×10^{-9}
1.01×10^0	9.71×10^{-9}	1.21×10^{-8}

Table 2 The sulfidation parabolic constants K_p of the tested alloys

Alloys	K_p /g ² ·cm ⁻¹ ·s ⁻¹		
	700°C	800°C	900 °C
Fe-25Cr-5Al	3.64×10^{-9}	2.01×10^{-8}	7.71×10^{-8}
Fe-25Cr-10Al	1.20×10^{-9}	2.98×10^{-9}	1.87×10^{-9}
Fe-25Cr	1.03×10^{-8}	2.99×10^{-7}	1.52×10^{-7}

To compare with Fe-25Cr, Fig. 3 shows the SEI of the surface morphologies and the cross section of sulfide scale on the Fe-25Cr alloy. It can be seen from Fig. 3 that the surface sulfide on Fe-25Cr was composed of large equiaxed grains. It contained predominantly S and Fe. The Cr content was very low. The sulfide scale on Fe-25Cr consisted of two uniform layers and an inter-

nal sulfidation zone. was much thicker than that on the Fe-25Cr-5Al or -10Al alloy. The external sulfide on Fe-25Cr was comprised of Fe₁₋₂S and FeCr₂S₄.

3.3 EPMA Results

Fig. 4 shows the elemental distribution images of the cross section of sulfide scale on the Fe-25Cr-10Al alloy. It can be seen that there were three sub-layers in the sulfide scale. The outer one was of the flake shape and contained S, Cr and Fe (from high to low). The intermediate layer contained S, Al, Cr and trace Fe. The inner layer was very thin, its composition was S and Al, being the same as that of the internal sulfide.

4 DISCUSSION

4.1 Sulfide Structure and Sulfidation Mechanism

A sulfide scale model (Fig. 5) of the Fe-Cr-Al alloy is proposed on the basis of analysis of XRD, EDAX and EPMA. According to the model in Fig. 5 the basic sulfidation process of the Fe-25Cr-*x*Al alloy is concluded as follows. In the initial period of sulfidation Al is sulfidized preferentially. In

Fig. 2 The surface morphologies of sulfide scales on the Fe-25Cr-5Al and -10Al alloys corroded at 800 °C and 1 Pa sulfur pressure for 120 min
 · (a)—Fe-25Cr-5Al; (b)—Fe-25Cr-10Al

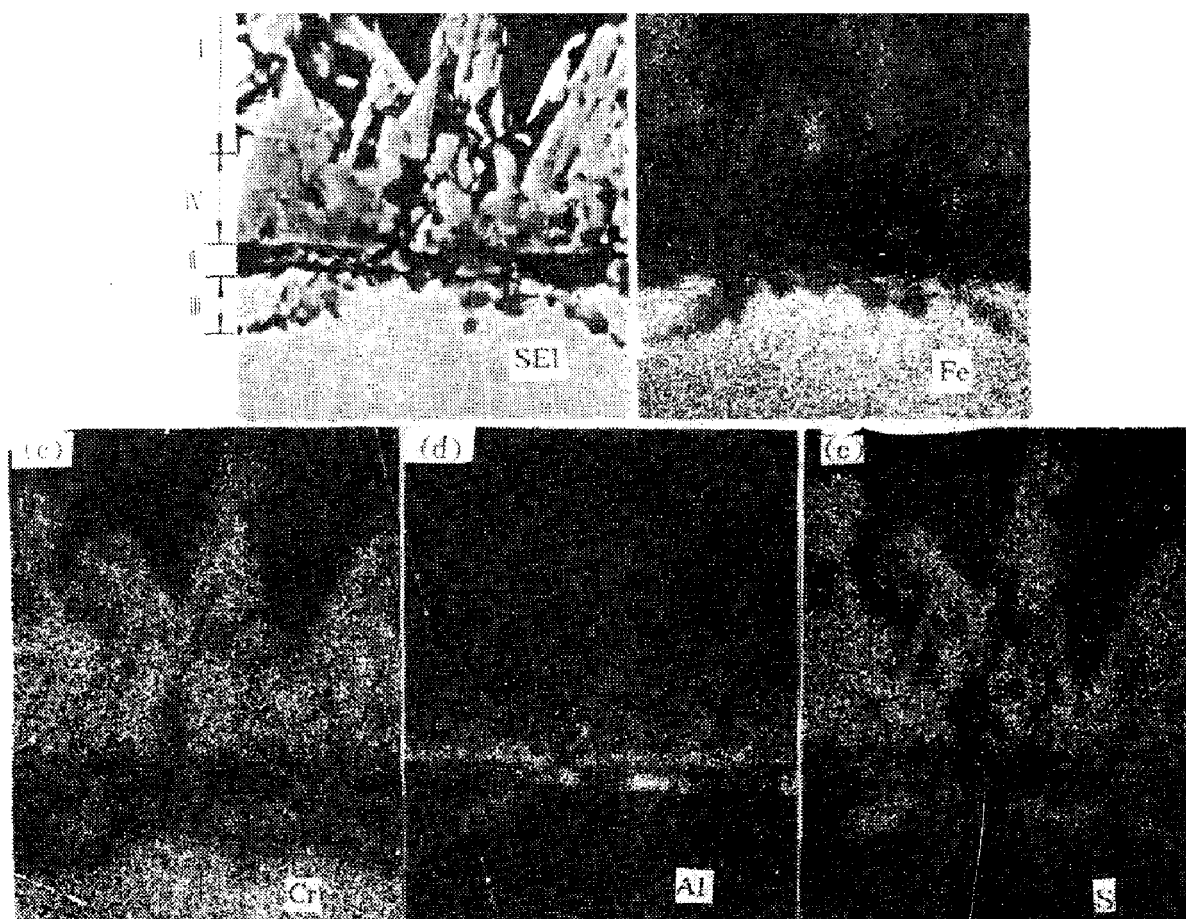


Fig. 4 The elemental distribution images by EPMA of the sulfide scale on Fe-25Cr-10Al corroded at 900 °C and $P_{S_2} = 10^{-1}$ Pa for 120 min

I —outer-layer; II —inner layer; III — internal sulfidation zone; IV —intermediate-layer

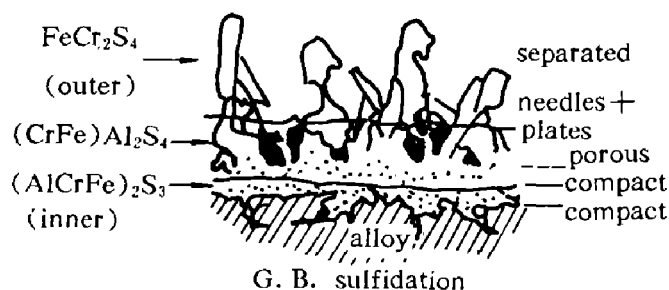


Fig. 5 A sulfide scale structure model of the Fe-Cr-Al alloy

the meantime Cr and Fe enrich and diffuse outwards. The affinity to S of Cr is larger than Fe, so Cr_2S_3 forms in advance of the iron sulfide. Meanwhile, the Al_2S_3 scale is destroyed and become the doped phase $(\text{AlCrFe})_2\text{S}_3$. Subsequently, Fe diffuses through Cr_2S_3 and forms FeCr_2S_4 spinel phase. With the going on of the reaction, Al also diffuses outwards and S transports inwards through crevices, pores and the sulfide phase, thus resulting in the continuous formation of Al_2S_3 through the reaction of Al with S.

4.2 Sulfidation Kinetics

The results in Fig. 1 indicate that the sulfidation kinetics of both 5Al and 10Al bearing alloys obey an incubation + parabolic law. This is consistent with the result by other authors on the sulfidation of the Fe-Cr-Al alloy^[8,9]. The only difference is that the sulfide rate of Fe-25Cr-10Al becomes larger with time. Through the study on the sulfide morphologies and structure for a short reaction time, it is considered that this difference relies on the growth of the sulfide scale. In the incubation period a thin and compact Al_2S_3 scale forms on the alloy surface. Afterwards, Cr and Fe diffuse through it leading to the corrosion kinetics enters the first parabolic law. As a result, the compactness and the protection of Al_2S_3 are destroyed. The formation of Cr_2S_3 phase

occurs, and thereby the diffusion of Fe and Cr in Cr_2S_3 becomes the controlling step. Because of Cr_2S_3 is of a higher defect concentration than Al_2S_3 , the resistance of sulfide to the diffusion of metal ions becomes smaller and the parabolic constant increases. So the curve enters the second parabolic law. At this time the outer sulfide is FeCr_2S_4 . It can be inferred that along with the increase of temperature and the extension of time the third parabolic law may be appears. This will reflect the growth of Fe_{1-x}S . The reaction kinetics curve for 900 °C in Fig. 1(c) proves this. Only S and Fe are detected by EDAX on the corresponding sample.

The sulfidation kinetics of the 5Al bearing alloy at high sulfur pressures and high temperatures is not very regular. An important reason is that the sulfide scale detaches from the alloy base and cracks during sulfidation. Under the experimental conditions the growth stress and the thermo-stress of the sulfide scale on Fe-25Cr-5Al are very high. The cracking and the separating of the outer sulfide from the alloy base occur in the furnace cooling process. This reason results in that the weight-gain curves of Fe-25Cr-5Al is not so regular as those of Fe-25Cr-10Al. In one hand the sulfidation kinetics deviate from the parabolic law. In the other hand, the sulfidation rate is no longer consistent with P_{S_2} . Besides, the sulfides formed at different steps are of different levels of defect concentration also affects the deviation of sulfidation kinetics.

It can be seen from Table 2 that the second parabolic constants of Fe-25Cr are decreased by one to two orders of magnitude by the addition of aluminium. The higher the temperature, the larger the difference. The thin Al_2S_3 scale formed in the initial period of sulfidation is rather protective. Although destroyed at last, a $(\text{CrFe})\text{Al}_2\text{S}_4$ in-

intermediate layer forms by the outward diffusion of Al. The doping of Al^{3+} can decrease the defect concentration of FeCr_2S_4 and increase the diffusion resistance of Cr^{3+} , especially Fe^{2+} . A 5 wt.-% Al is relatively small and the amount of Al_2S_3 phase is very little. No complete protective scale forms on the 5 Al containing alloy.

5 CONCLUSIONS

(1) The sulfidation of Fe-25Cr-5Al and -10Al alloys follow basically the parabolic law. The addition of aluminium to Fe-25Cr decreases its sulfidation rate by one to two orders of magnitude. The effect of 10 Al is larger than that of 5 Al.

(2) Two or more parabolic laws appear in the sulfidation kinetics of the 10Al bearing alloy and the parabolic constant increases with time. It has a close relationship to the formation process and order of sulfide layers in the scale.

(3) The addition of aluminium changes the structure and the nature of sulfide scale for Fe-25Cr. The formation of Al_2S_3 in the early period of reaction and the decreasing of the defect concentration of sulfide by the doping of Al^{3+} to Cr_2S_3 or $(\text{CrFe})_2\text{S}_3$ reduce the sulfidation rates of Fe-25Cr.

REFERENCES

- 1 Zuo, Y. Petrochemical Corrosion and Protection, 1988, 19; 12.
- 2 Mrowec, S *et al.* Oxid Met., 1969, 1; 93.
- 3 Narita, T *et al.* Oxid Met., 1981, 21; 39.
- 4 Narita, T *et al.* Oxid Met., 1981, 21; 57.
- 5 Qi, H B *et al.* J of University of Science and Technology Beijing, in print.
- 6 Zalenko, P D *et al.* Oxid Met., 1971, 8; 313.
- 7 Mrowec, S *et al.* Oxid Met., 1979, 13; 710.
- 8 Narita, T *et al.* Oxid Met., 1981, 22; 181.
- 9 Saxena, D *et al.* Oxid Met., 1987, 18; 127.
- 10 Qi, H B *et al.* In: Proc of the 7th APCCC, Vol. 1, 1991, 1; 118.